

Study on the induction period of methane aromatization over Mo/HZSM-5: partial reduction of Mo species and formation of carbonaceous deposit

Hui Jiang, Linsheng Wang, Wei Cui and Yide Xu*

State Key Laboratory of Catalysis, Dalian Institute of Chemical Physics, Chinese Academy of Sciences, Dalian 116023, PR China

Received 29 September 1998; accepted 23 December 1998

The induction period of dehydrogenation and aromatization of methane over Mo/HZSM-5 was studied by combining a pulse reaction method with TPSR, UV laser Raman, and ^{13}C CPMAS NMR techniques. BET and XRD results showed that Mo species were well dispersed on/in the zeolite. TPSR in CH_4 stream revealed that Mo species were reduced in at least two different stages before the formation of benzene. TPR results were in agreement with TPSR results. The two stages might be attributed to the reduction of two kinds of Mo^{6+} species to low valence Mo species. One was polymolybdate MoO_3 , and the other was crystalline MoO_3 . UV Raman spectra showed the existence of octahedrally coordinated polymolybdate species. XRD, however, did not detect any crystalline MoO_3 , possibly because they were too small to be detected with this technique. Pulse reaction results indicated that pre-reduction of the catalyst and formation of carbonaceous deposit could shorten the induction period. It is concluded that the formation of active sites during the induction period via partial reduction of Mo^{6+} species and formation of carbonaceous deposit on partially reduced Mo species is of significance for methane aromatization over Mo/HZSM-5.

Keywords: methane aromatization, induction period, Mo species, partial reduction, carbonaceous deposit

1. Introduction

The conversion of methane to more useful high hydrocarbons not only is a great challenge to catalytic chemists, but also has great significance to industrial utilization of natural gas. For the past nearly twenty years, the oxidative coupling of methane (OCM) was under intensive research in the world [1,2]. Although a great number of advances have been made, many difficulties and problems still remain to be solved before its industrial application. Therefore, many researchers left this field and moved to other subjects. Recently, great efforts have been devoted to the partial oxidation of methane for the production of syngas and the dehydrogenation and aromatization of methane under non-oxidative conditions [3–16]. For the latter reaction, Wang et al. [17] first reported that methane could be selectively converted to aromatics without using oxidant over a Mo-modified HZSM-5 zeolite catalyst. To date, quite similar catalytic performances have been reported by several research groups for methane aromatization over Mo/HZSM-5 catalysts, and, therefore, the reaction has been well established. As far as the active sites and/or reaction mechanism is concerned, however, there are some discrepancies among various researchers. Previously, Xu et al. [4] proposed a mechanism in which both the heterolytic splitting of methane in a solid acid environment and a molybdenum carbene-like complex as an intermediate were of significance. The molybdenum carbene-like complex then dimerized to form ethylene as the primary product. Later, they

further suggested that the active center be partially reduced molybdenum oxide species $\text{MoO}_{(3-x)}$ [8]. Lin et al. [10] supposed that the activation of methane to form $\text{CH}_3\cdot$ free radicals occurred via a synergistic action between MoO_x and the Brønsted acid sites, and then the $\text{CH}_3\cdot$ radicals dimerized to form ethane as the primary product. Lunsford et al. [11] noted that Mo_2C was formed after the reaction through their XPS characterization. They suggested that methane be initially activated on the sites of Mo_2C within the zeolite channels to produce ethylene (and H_2) as the sole primary product which reacted further on acid sites to form the final aromatic products. Solymosi et al. [13–16] investigated methane activation over various unsupported and supported molybdenum compounds and concluded that Mo_2C – MoO_2 with an oxygen deficiency was responsible for the production of ethylene from methane, and ethylene was then converted to benzene on the acid sites of the HZSM-5 support [15]. Lately, Lunsford et al. [12] suggested that coke-modified Mo_2C surface be the active center for the reaction, because pre-formation of Mo_2C on the support with no coke deposit could not completely eliminate the induction period.

Despite the different points of view put forward by many researchers, it is commonly accepted that there is an induction period in the early stage of the reaction of methane aromatization over Mo/HZSM-5. Pulse reaction is an effective and suitable technique for monitoring the induction period. In this work, we report the results obtained from pulse reaction and other techniques, such as temperature-programmed surface reaction (TPSR),

* To whom correspondence should be addressed.

temperature-programmed reduction (TPR), ultra-violet laser Raman spectrometer (UV LRS) and ^{13}C cross polarization magic angle spinning NMR (^{13}C CPMAS-NMR). In order to understand and get an insight into the induction period of the reaction, we pay more attention to the partial reduction of Mo species and the location of carbonaceous deposit.

2. Experimental

2.1. Catalyst preparation

NaZSM-5 ($\text{SiO}_2/\text{Al}_2\text{O}_3 = 25$) zeolite was supplied by Nankai University. It was first converted into ammonium form by repeated ion exchange with a 1 mol/l NH_4NO_3 aqueous solution at about 371 K (4 times and each time for 1 h) and then dried at 333 K for 1.5 h and 393 K for 4 h. HZSM-5 was prepared by calcining $\text{NH}_4\text{ZSM-5}$ at 773 K for 6 h, and was denoted as HZ. Mo/HZSM-5 was prepared by impregnating $\text{NH}_4\text{ZSM-5}$ with desirable amount of ammonium heptamolybdate (AHM) aqueous solution at room temperature for 24 h. It was then dried at 393 K for 4 h and calcined at 773 K for 6 h. The catalysts used in this research were with nominal Mo loading of 2 and 10%, and were denoted as 2Mo/HZ and 10Mo/HZ separately. All catalysts were pressed, crushed and sorted into size of 20–60 mesh.

2.2. Pulse reaction

Pulse reaction was carried out on a self-made apparatus. The catalyst of 0.1 g was heated under He stream to 973 K in 50 min and maintained at 973 K for 1 h. Then methane or other gas pulse was introduced. The outlet gas was analyzed by a Shimadzu GC-9A gas chromatograph using TCD as the detector. The volume of one pulse was about 1.3 ml. The conversion of methane and the yield of product were calculated on the basis of carbon number balance in gas phase. CH_4 and C_2H_6 used in this work were with high purity of 99.99%.

2.3. Catalyst characterization

TPSR was carried out in a quartz tubular micro-flow reactor containing 0.2 g catalyst, using a TE-150 multi-channel mass spectrometer to record signals. The catalyst was heated to 873 K in He stream at a heating rate of 15 K/min and maintained at 873 K for 30 min and then cooled down to room temperature. It was then heated to 973 K at 15 K/min in CH_4 stream. In order to monitor the change at around 973 K clearly, the catalyst was then slowly heated from 973 to 983 K in 30 min (at a heating rate of about 0.33 K/min).

TPR was carried out on a conventional self-made apparatus. The sample was placed in a quartz reactor and flushed with Ar stream. It was heated to 873 K at a heating rate of 10 K/min and maintained at 873 K for 30 min

and then cooled down to room temperature. It was then reduced under H_2/Ar (5 vol% of H_2) stream with a flow rate of 20 ml/min and heated from room temperature to 1173 K at a heating rate of 10 K/min.

UV laser Raman spectra were recorded on a home-made spectrometer. A 244 nm line from an Innova 300 FRED Ar^+ laser was used as the excitation source. The laser power at the samples was 5 mW. Samples were mounted into a spinning holder to avoid thermal damage during scanning. The spectral resolution was estimated to be 1.0 cm^{-1} .

X-ray powder diffraction patterns were obtained on a Rigaku diffractometer using $\text{Cu K}\alpha$ radiation at room temperature. Powder diffractograms were recorded over a range of 2θ values from 5 to 50° at a scanning rate of $8^\circ/\text{min}$. The condition was 40 kV and 500 mA. All the patterns could be processed with a computer system.

Specific surface area and pore volume of the samples was obtained by the BET method at liquid-nitrogen temperature with a Micromeritics ASAP-2000 instrument. All the data were collected and processed by an IBM computer.

^{13}C cross polarization magic angle spinning NMR (^{13}C CPMAS-NMR) experiments were performed on a Fourier transform NMR spectrometer (Bruker DRX-400) equipped with a Chemagnetic solids accessory. A spin rate of 6 kHz and 90° pulses of $4.7\text{ }\mu\text{s}$ were employed, and chemical shifts were referenced to tetramethylsilane.

3. Results and discussion

3.1. Reduction of Mo species in the induction period

Figure 1 shows the TPSR results of methane over 2Mo/HZ and 10Mo/HZ catalysts. The response curves of CO_2 and H_2O had double peaks, which implied that Mo^{6+} species were reduced by two stages. In the first stage, methane interacted with Mo species to evolve CO_2 , H_2O and CO. In the second stage, a large amount of CO and a little of CO_2 and H_2O were produced simultaneously (note the sensitivities for different species are different). Neither C_2H_4 nor C_6H_6 could be detected in these two stages. C_2H_4 and C_6H_6 could only be evolved and became more and more after the disappearance of CO_2 evolution, while the evolution of CO and H_2O could still be detected. Since the reaction was carried out under non-oxidative conditions (no other oxygen sources in the gas phase), Mo species, which are coordinated with oxygen species, were the only oxygen source to be used to produce CO_2 , CO and H_2O . Thus, we suggest that the induction period before the initial formation of benzene closely relate to the gradual reduction of Mo species. Namely, it is the Mo species which are not in a high valence state (Mo^{6+}), but in a lower valence state that may be responsible for the conversion of methane to ethylene and benzene. We also notice in the TPSR profiles that for the 2Mo/HZ sample (figure 1(a)), the two peaks have some overlap; however, for the 10Mo/HZ sample (figure 1(b)), the two peaks are obviously discrete. The

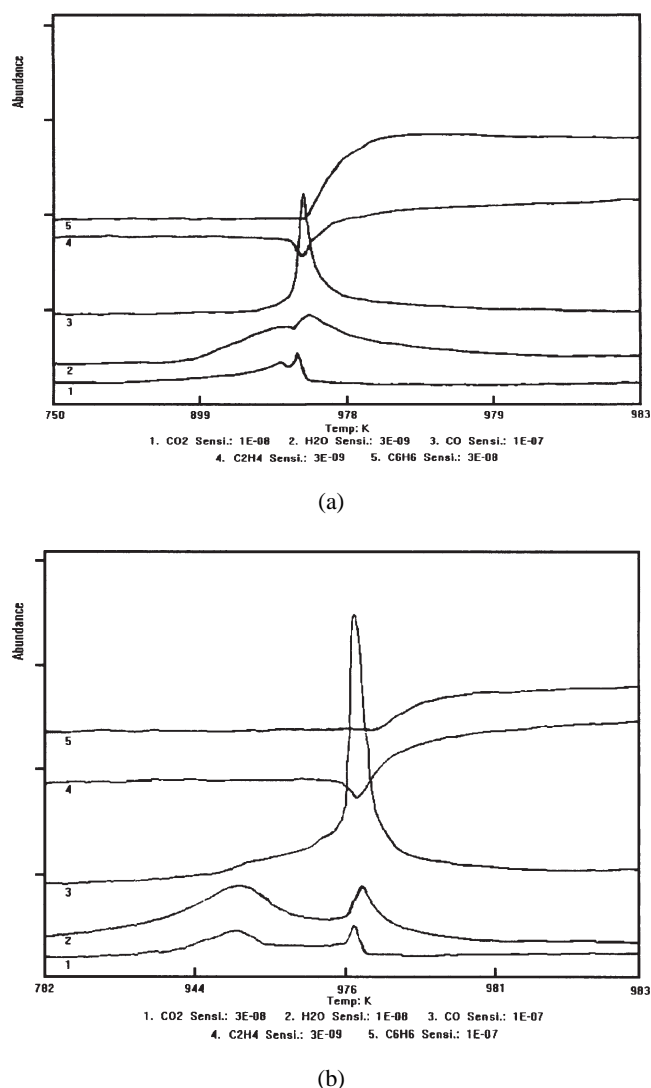


Figure 1. TPSR results of various catalysts with different Mo loadings. (a) 2Mo/HZ; (b) 10Mo/HZ.

TPSR results lead us to the conclusion that reduction of Mo species (Mo^{6+}) is necessary for the formation of active sites available for methane aromatization.

Figure 2 shows the TPR profiles of various catalysts. For HZ almost no reduction peak could be recorded in the TPR profile. For 2Mo/HZ, however, there were a small reduction peak at about 750 K and a second reduction peak well developed at 923 K. If the temperature ran higher than 1073 K, a third reduction peak would develop. For 10Mo/HZ, there were two reduction peaks: one was at about 750 K and the other at about 923 K. These two peaks were clearly discrete. In the same way, the third reduction peak would develop if the temperature ran higher than 1073 K. It is interesting to notice that there are some similarities between TPR and TPSR profiles.

The TPR profiles of supported MoO_3 catalysts have been extensively studied [18]. In their TPR profiles of impregnated $\text{MoO}_3/\gamma\text{-Al}_2\text{O}_3$, the authors found that there were three peaks for the high Mo-loading catalyst. It was suggested that the first peak be attributed to the reduction of polymolybdate MoO_3 to MoO_2 , and the second to the reduction of crystalline MoO_3 to MoO_2 . Meanwhile, the third peak appearing at the highest temperature was assigned to the reduction of MoO_2 to Mo. Referring to these results obtained from $\text{MoO}_3/\gamma\text{-Al}_2\text{O}_3$ samples, we assumed that the status of Mo species on Mo/HZ were similar to those on $\text{MoO}_3/\gamma\text{-Al}_2\text{O}_3$ samples. This was supported by the UV Raman spectra of Mo/HZ catalysts. As we can see from figure 3, the spectra recorded from the 2Mo/HZ and 10Mo/HZ samples (spectrum (b) and (c)) exhibit the bands at about 850, 958 and 1881 cm^{-1} . These bands are characteristic for Mo species in octahedrally coordinated polymolybdate form, as Williams et al. [19,20] reported. The bands at around 380 and 1628 cm^{-1} are due to the HZ support (figure 3(a)).

The XRD patterns of relevant samples are shown in figure 4. Even for the 10Mo/HZ catalyst, the pattern was similar to that of HZ, only showing the characteristic peaks

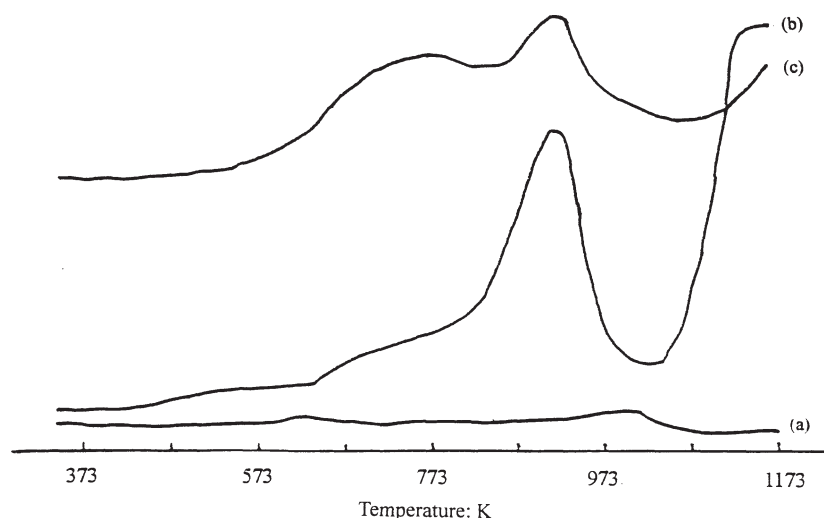


Figure 2. TPR profiles of various catalysts with different Mo loadings. (a) HZ (100 mg); (b) 2Mo/HZ (250 mg); (c) 10Mo/HZ (51 mg).

of HZ with the main 2θ values of about 8, 9 and 23–25°. No MoO_3 crystallites could be detected. This may be an indication that MoO_3 crystallites are highly dispersed on HZ and the particle size is smaller than 4 nm so that they cannot be detected by XRD technique.

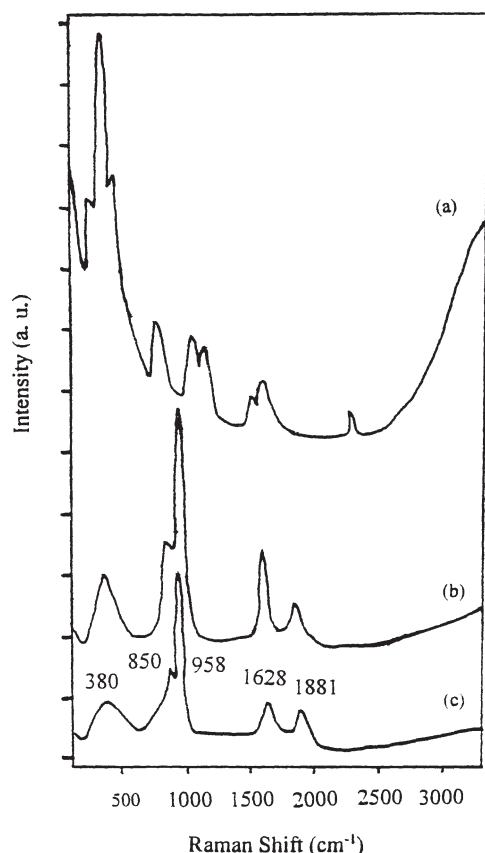


Figure 3. UV Raman spectra of various catalysts with different Mo loadings. (a) HZ; (b) 2Mo/HZ; (c) 10Mo/HZ.

In addition, table 1 lists the BET results. Even for the 10Mo/HZ sample, the surface area was 312 m^2/g and the micro-pore volume was 0.11 ml/g , compared with the surface area of 385 m^2/g and micro-pore volume of 0.13 ml/g for the HZ sample. These again imply that Mo species are well dispersed on the zeolite.

To sum up, it is assumed that there are two kinds of Mo^{6+} species on the as-prepared Mo/HZ catalyst. One is in the form of octahedrally coordinated polymolybdate, and the other is in the form of crystalline MoO_3 with the particle size less than 4 nm. In CH_4 stream at 973 K, both Mo^{6+} species were reduced to some low valence Mo species. These reduced Mo species may be necessary for the formation of the active sites for methane aromatization.

3.2. Pulse reaction study of the induction period

Figure 5 shows the pulse reaction results over HZ. The products in the tail-gas were CO , CO_2 , C_2H_4 and C_2H_6 (C_2H_6 was not shown in the figure), and we could not detect C_6H_6 even at the 15th pulse. In the early stage, with the increase in number of pulses, the conversion of CH_4 and the yield of CO_x decreased quickly. Over 2Mo/HZ and 10Mo/HZ catalysts, things changed a lot (figures 6 and 7). The methane conversion increased with number of pulses in the early stage and reached its maximum at the 4th pulse

Table 1
BET surface area and pore volume of various catalysts with different Mo loading.

Sample	Surface area (m^2/g)	Micro-pore volume (ml/g)
HZ	384.6	0.13
2Mo/HZ	356.5	0.12
10Mo/HZ	311.9	0.11

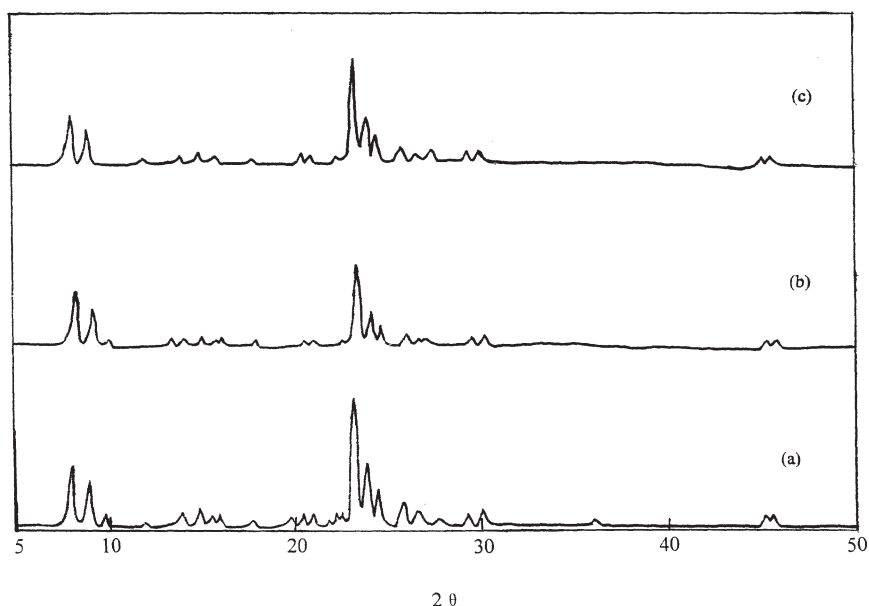


Figure 4. XRD patterns of various catalysts with different Mo loadings. (a) HZ; (b) 2Mo/HZ; (c) 10Mo/HZ.

on 2Mo/HZ and at the 7th pulse on 10Mo/HZ. Then the methane conversion fell quickly. For the 2Mo/HZ catalyst, the methane conversion fell to about 4%; while for 10Mo/HZ, it fell to 3%. It then increased slowly. The CO yield on the 2Mo/HZ and 10Mo/HZ catalysts followed the same change as the methane conversion did, except that it fell continuously after reaching the maximum. It is interesting to notice that as soon as the methane conversion reached its maximum and started to fall, the yield of CO₂ fell to zero and the evolution of C₂H₄ and C₆H₆ began. Therefore, the stage of the sharp increase in methane conversion may relate to the gradual reduction of Mo⁶⁺ species. For 2Mo/HZ catalyst (figure 6), only after 4 methane pulses were C₂H₄

and C₆H₆ evolved; while for 10Mo/HZ catalyst (figure 7), about 13 methane pulses were needed before the evolution of C₂H₄ and C₆H₆ could be detected. All these results are in agreement with corresponding results obtained in TPSR experiments.

To get more information about the induction period, we used H₂ or C₂H₆ pulses to pretreat the 10Mo/HZ catalyst before introducing the CH₄ pulses. The results are presented in figures 8–10 and table 2. After pretreating the catalyst with 20 H₂ pulses, only 5 CH₄ pulses were needed on the 10Mo/HZ catalyst for the evolution of C₂H₄ and C₆H₆, as we can see from table 2 and figure 8. This suggests that pretreating with H₂ pulses can reduce some Mo⁶⁺ species so that they can be reduced by less CH₄ pulses. It is more interesting if we pretreated the 10Mo/HZ catalyst with 3 C₂H₆ pulses. We found that C₂H₄ and C₆H₆ immediately evolved as soon as CH₄ pulse was introduced. Figure 9 presents the result. In comparison with the result obtained by pretreating 10Mo/HZ with 20 H₂ pulses, the yield of C₆H₆ was higher and that of CO was lower, so it is reasonable to suppose that Mo⁶⁺ species only need to be partially reduced to form the active sites. Surprisingly, when we pretreated the 10Mo/HZ catalyst with 10 C₂H₆ pulses, methane pulse reaction nearly reached a steady period starting from

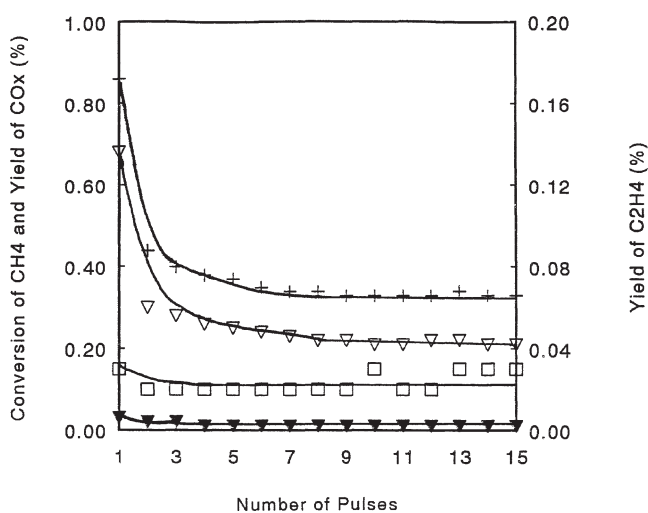


Figure 5. Dependence of methane conversion and product yield on number of pulses over HZ. (+) Conversion of CH₄; (∇) yield of CO; (▼) yield of CO₂; (□) yield of C₂H₄.

Table 2
Pulse reaction results of methane over Mo/HZ catalysts.

Catalyst	Pretreatment	Pulse(s) needed for C ₆ H ₆ formation
2Mo/HZ	No	4
10Mo/HZ	No	13
	20 H ₂ pulses	5
	3 C ₂ H ₆ pulses	1
	10 C ₂ H ₆ pulses	1

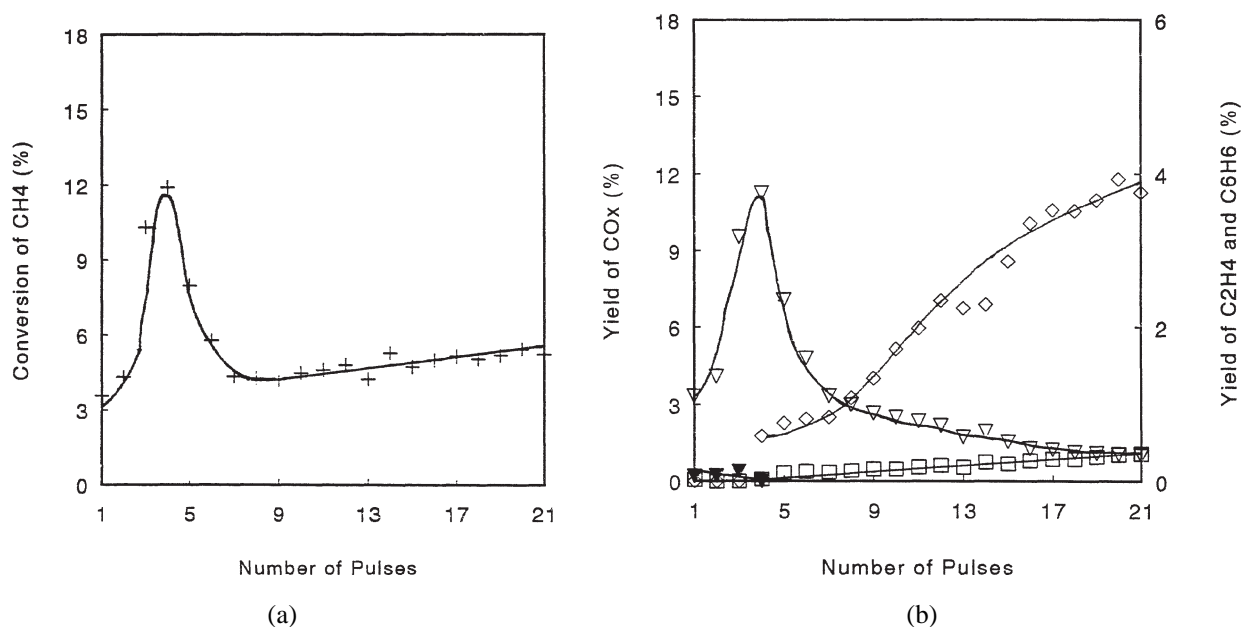


Figure 6. (a) Dependence of methane conversion on number of pulses over 2Mo/HZ. (b) Dependence of product yield on number of pulses over 2Mo/HZ. (∇) Yield of CO; (▼) yield of CO₂; (□) yield of C₂H₄; (◇) yield of C₆H₆.

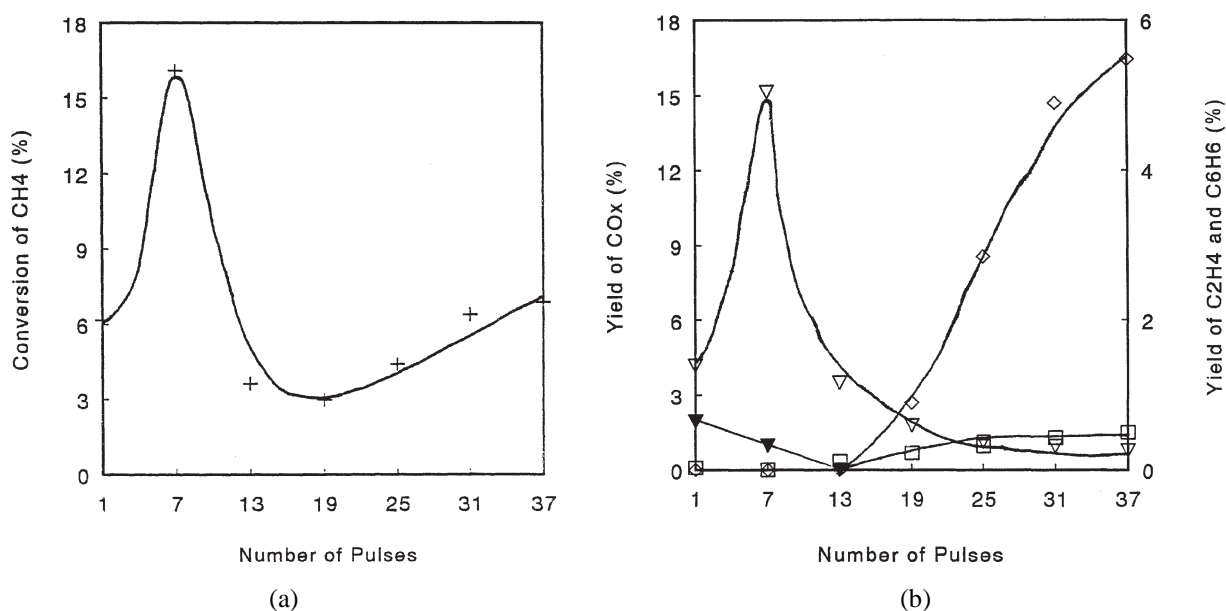


Figure 7. (a) Dependence of methane conversion on number of pulses over 10Mo/HZ. (b) Dependence of product yield on number of pulses over 10Mo/HZ. After 1 pulse was introduced and signal was recorded, 5 pulses were introduced continuously without recording signals. (∇) Yield of CO; (\blacktriangledown) yield of CO₂; (\square) yield of C₂H₄; (\diamond) yield of C₆H₆.

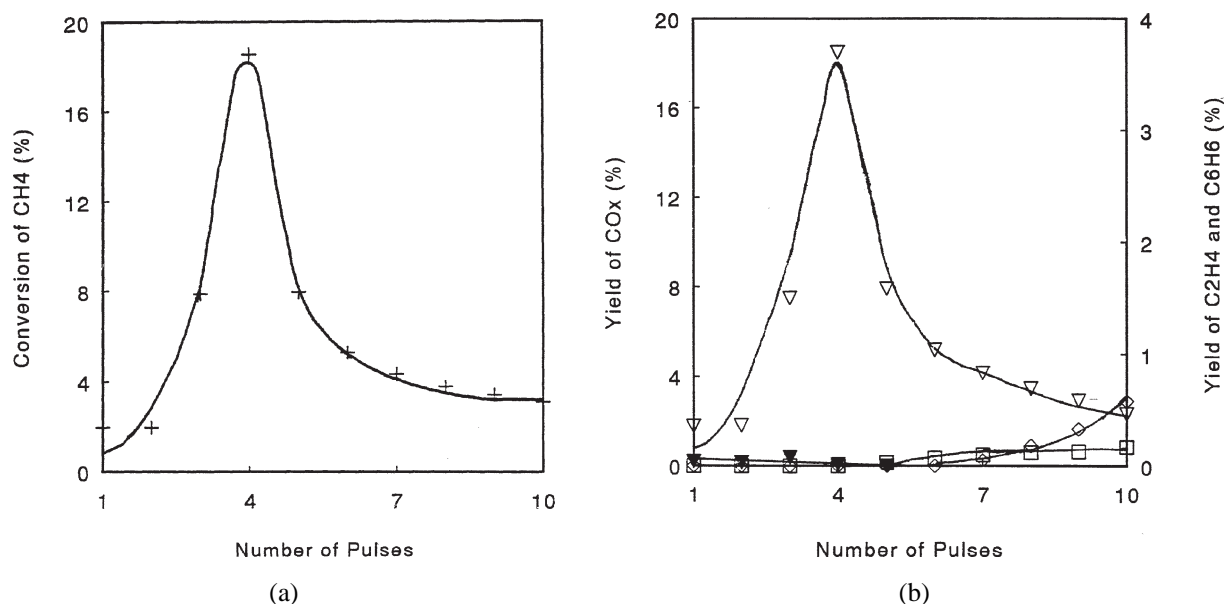


Figure 8. (a) Dependence of methane conversion on number of pulses over 10Mo/HZ pretreated with 20 H₂ pulses. (b) Dependence of product yield on number of pulses over 10Mo/HZ pretreated with 20 H₂ pulses. (∇) Yield of CO; (\blacktriangledown) yield of CO₂; (\square) yield of C₂H₄; (\diamond) yield of C₆H₆.

the second pulse and showed no induction period again (figure 10). For the first CH₄ pulse, we could get even higher methane conversion and benzene yield. This implies that the induction period of methane aromatization over Mo/HZ catalyst has a more direct relation to carbonaceous deposit than to the partial reduction of Mo species.

3.3. Characterization of carbonaceous deposit by ¹³C CPMAS NMR

The carbonaceous species from methane aromatization over HZ and Mo/HZ at 973 K for about 6 h were character-

ized by a ¹³C CPMAS-NMR spectrometer. The recorded spectra are presented in figure 11. A wide NMR band at chemical shift of about 10–40 ppm appeared on both HZ and Mo/HZ. This band is attributed to a carbonaceous deposit formed on the acid sites of HZ zeolite. An additional NMR band at chemical shift of about 130 ppm was recorded only on the Mo/HZ catalyst. No such band could be detected on the HZ sample. This carbonaceous deposit should be related to Mo species. Therefore, there are two kinds of carbonaceous species formed on the Mo/HZ catalyst in the reaction. One is located on acid sites, and the other is located on Mo species. The latter should be ben-

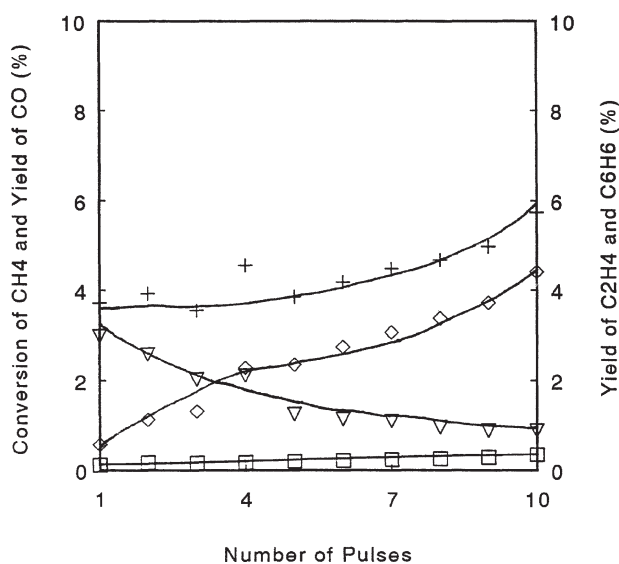


Figure 9. Dependence of methane conversion and product yield on number of pulses over 10Mo/HZ pretreated with 3 C₂H₆ pulses. (+) Conversion of CH₄; (∇) yield of CO; (□) yield of C₂H₄; (◇) yield of C₆H₆.

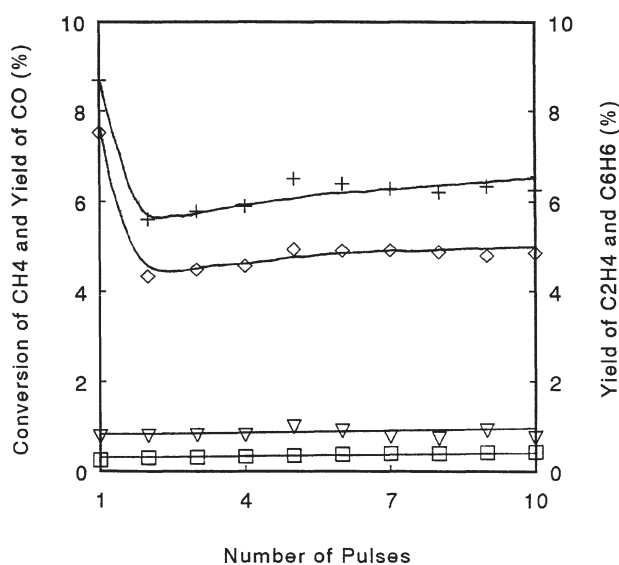


Figure 10. Dependence of methane conversion and product yield on number of pulses over 10Mo/HZ pretreated with 10 C₂H₆ pulses. (+) Conversion of CH₄; (∇) yield of CO; (□) yield of C₂H₄; (◇) yield of C₆H₆.

eficial to the titled reaction. It could be due to Mo₂C, as Lunsford et al. [11,12] and Solymosi et al. [14–16] suggested, as well as to an amorphous carbonaceous species associated with partially reduced Mo species. Further research on carbonaceous deposit on Mo/HZ catalyst is necessary to characterize its nature and to understand its role in methane aromatization.

Concluding all the results above, we may explain the induction period of the titled reaction as follows. At the beginning, methane interacts with Mo⁶⁺ species on the surface of the catalyst to produce H₂O and CO₂/CO, and Mo⁶⁺ may be partially reduced. Then some kind of carbonaceous deposit interacts with partially reduced Mo species to form active sites. The more active sites are formed, the higher

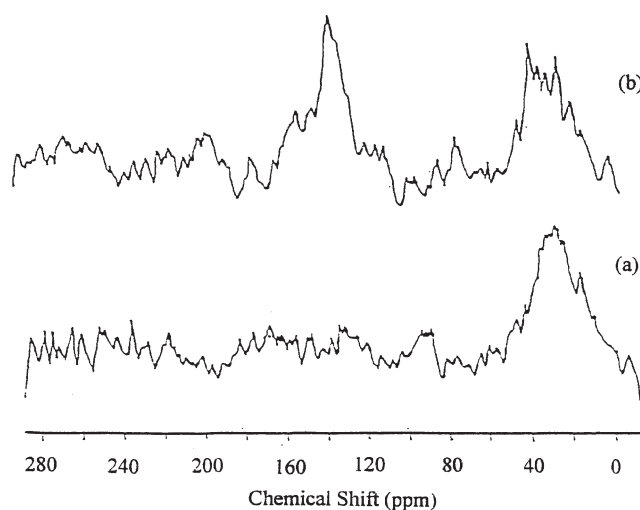


Figure 11. The ¹³C CPMAS-NMR spectra recorded from (a) HZ and (b) Mo/HZ.

the reactivity of CH₄ and the yield of C₂H₄ and C₆H₆ become. When the active sites are formed to a proper extent, the conversion of methane and the yield of benzene reach their optimum values, and this can be maintained for a period. Then, more carbonaceous deposit, either on the acid sites or on the partially reduced Mo species, will deactivate the catalyst, resulting in a decrease in methane conversion and benzene yield [10].

In conclusion, partial reduction of high valence Mo⁶⁺ species and formation of carbonaceous deposit on partially reduced Mo species may be the main steps in the induction period, during which the active sites are formed gradually. Carbonaceous deposit may play a more important role in the titled reaction.

Acknowledgement

The financial supports of the National Natural Science Foundation of China and China Petrochemical Corporation are gratefully acknowledged. We acknowledge Mr. Xianchun Liu for performing NMR experiments and Dr. Guang Xiong and Professor Can Li for performing UV Raman spectra experiments and discussing the results.

References

- [1] Y. Ono, Catal. Rev. Sci. Eng. 34 (1992) 179.
- [2] J.H. Lunsford, in: *Proceedings 10th International Congress Catalysis*, eds. L. Gucci, F. Solymosi and P. Tétényi (Akadémiai Kiadó, Budapest, 1993) p. 103.
- [3] V.R. Choudhary, A.K. Kinage and T.V. Choudhary, Science 275 (1997) 1286.
- [4] Y. Xu, S. Liu, L. Wang, M. Xie and X. Guo, Catal. Lett. 30 (1995) 135.
- [5] S.-T. Wong, Y. Xu, W. Liu, L. Wang and X. Guo, Appl. Catal. A 136 (1996) 7.
- [6] Y. Xu, W. Liu, S.-T. Wong, L. Wang and X. Guo, Catal. Lett. 40 (1996) 207.

- [7] L. Wang, Y. Xu, S.-T. Wong, W. Cui and X. Guo, *Appl. Catal. A* 152 (1997) 173.
- [8] Y. Shu, Y. Xu, S.-T. Wong, L. Wang and X. Guo, *J. Catal.* 170 (1997) 11.
- [9] L. Chen, L. Lin, Z. Xu, T. Zhang and X. Li, *Catal. Lett.* 39 (1996) 169.
- [10] L. Chen, L. Lin, Z. Xu, X. Li and T. Zhang, *J. Catal.* 157 (1995) 190.
- [11] D. Wang, J.H. Lunsford and M.P. Rosynek, *Topics Catal.* 3 (1996) 289.
- [12] D. Wang, J.H. Lunsford and M.P. Rosynek, *J. Catal.* 169 (1997) 347.
- [13] F. Solymosi, A. Erdöhelyi and A. Szöke, *Catal. Lett.* 32 (1995) 43.
- [14] A. Szöke and F. Solymosi, *Appl. Catal. A* 142 (1996) 361.
- [15] F. Solymosi, A. Szöke and J. Cserényi, *Catal. Lett.* 39 (1996) 157.
- [16] F. Solymosi, J. Cserényi, A. Szöke, T. Bánsági and A. Oszkó, *J. Catal.* 165 (1997) 150.
- [17] L. Wang, L. Tao, M. Xie, G. Xu, J. Huang and Y. Xu, *Catal. Lett.* 21 (1993) 35.
- [18] J.R. Regalbuto and J.-W. Ha, *Catal. Lett.* 29 (1994) 189.
- [19] C.C. Williams, J.G. Ekerdt, J.-M. Jehng, F.D. Hardcastle, A.M. Turek and I.E. Wachs, *J. Phys. Chem.* 95 (1991) 8781.
- [20] C.C. Williams, J.G. Ekerdt, J.-M. Jehng, F.D. Hardcastle and I.E. Wachs, *J. Phys. Chem.* 95 (1991) 8791.